RAPID COMMUNICATION

CrossMark

Room temperature ethanol sensor based on ZnO prepared via laser ablation in water

Takahiro Kondo[1,3†], Yoshihiro Sato[2†], Masahiro Kinoshita[2], Prabakaran Shankar[1*], Neli N. Mintcheva[1,4], Mitsuhiro Honda[1,5], Satoru Iwamori[2], and Sergei A. Kulinich[1*]

[1]Institute of Innovative Science and Technology, Tokai University, Hiratsuka, Kanagawa 259-1292, Japan
[2]Faculty of Engineering, Tokai University, Hiratsuka, Kanagawa 259-1292, Japan
[3]Department of Chemistry, Gakushuin University, Toshima, Tokyo 171-0031, Japan
[4]Department of Chemistry, University of Mining and Geology, Sofia 1700, Bulgaria
[5]Graduate School of Engineering, Nagoya Institute of Technology, Nagoya 466-8555, Japan

*E-mail: madanprabakar@gmail.com; skulinich@tokai-u.jp
†These authors contributed equally to this work.

The present work reports on room-temperature ethanol sensing performance of ZnO nanospheres and nanorods prepared using pulsed laser ablation in water. Nanosecond and millisecond lasers were used to prepare ZnO nanomaterials with hexagonal wurtzite crystal structure. The two contrasting nanostructures were tested as gas sensors towards volatile compounds such as ethanol, ammonia, and acetone. At room temperature, devices based on both ZnO nanomaterials demonstrated selectivity for ethanol vapor. The sensitivity of nanospheres was somewhat higher compared to that of nanorods, with response values of ∼19 and ∼14, respectively, towards 250 ppm. Concentrations as low as 50 ppm could be easily detected. © 2017 The Japan Society of Applied Physics

Detection of different impurities in the ambient atmosphere is a growing need to control air quality both indoors and outdoors. Metal oxide based chemiresistive gas sensors have been increasingly used to detect gases/vapors, often demonstrating high selectivity and sensitivity, biocompatibility and low cost.[1–8] As gas-sensing performance of chemiresistive sensors is highly dependent on their surface area and morphology, numerous nanostructures (mainly of metal oxides, ZnO, SnO$_2$, WO$_3$, and In$_2$O$_3$[1–8]), such as nanoparticles (NPs), nanorods, nanowires, nanoflowers, nanosheets, nanoflakes, and so on, have been actively studied in order to establish relationships between nanomaterial chemistry, surface state and morphology, and its efficiency for gas detection.[1–8]

Laser ablation in liquid (LAL) is a convenient technique to produce NPs at laboratory scales.[9–16] In this approach, laser beam is typically focused on a metal target, producing plasma, vapor or molten metal drops which then react with the liquid and give rise to NPs.[10–16] The approach is easy to operate, environmentally friendly and permits to prepare a large number of diverse metal, oxide, sulfide, and carbide NPs.[9–16] It is also known for its extremely high temperature gradient and quenching rates in the reaction zone, which often leads to the formation of metastable phases of various nanomaterials.[9,11,13,14]

Though as a preparation technique LAL conveniently provides various nanostructures of metal oxides/sulfides with different morphologies, to date, LAL-produced nanomaterials were seldom tested in gas-sensing devices.[9,15] Xiao et al. reported alcohol sensing by porous WO$_3$ nanoflakes prepared via aging LAL-generated colloids,[15] while promising acetone and ethanol sensing was demonstrated by hollow ZnS NPs prepared by means of a millisecond laser.[9] Finally, Goto et al. exhibited the ability of oxygen adsorption on LAL-prepared ZnO NPs under various partial pressures, thus opening avenue for ZnO nanomaterials generated by LAL as potential gas sensors.[17] Yet, no work on gas sensing performance of LAL-prepared ZnO nanomaterials was reported thus far. Meanwhile, ZnO nanostructures prepared by electrospinning,[8] sputtering,[18,19] thermal oxidation,[20] and spray pyrolysis[21–23] showed response to ethanol at room

temperature. Therefore, in the present work, we aimed at testing ZnO nanostructures (nanorods and nanospheres) prepared by LAL as gas-sensing devices towards volatile organic compounds such as ethanol, ammonia and acetone at room temperature. High response towards ethanol, as well as good selectivity, was observed.

Millisecond (ms) and nanosecond (ns) pulsed lasers (Nd:YAG type with wavelength 1064 nm) were used to ablate zinc metal for 30 min in water medium (15 mL) and the beam was applied horizontally through a quartz cuvette wall. For ms-laser, the optimized parameters such as pulse peak power, width, and frequency were 4 kW, 1.0 ms, and 5 Hz, respectively. For ns-laser, the applied parameters, such as pulse width, energy, and frequency were 7 ns, 100 mJ/pulse, and 10 Hz, respectively. Upon ablation for 30 min, the ZnO colloids were collected onto Cu grids, Si substrates, or interdigitated electrodes, after which they were used for characterization and sensing studies.

The prepared colloids were characterized with X-ray diffractometry (XRD) and transmission electron microscopy (TEM). To prepare gas sensors, as-produced fresh colloids were drop-cast onto commercial interdigitated electrodes (with gap 5 μm, from DropSens). In order to achieve thick films, five layers of corresponding colloid (30 μL each time) were subsequently drop-cast and evaporated on each electrode (at 50 °C). To stabilize the sensors, prior to tests they were annealed in air at 400 °C for 2 h.

Gas sensing performance towards ethanol, ammonia, and acetone was studied using an acrylic chamber (5.4 L) equipped with a fan and electrometer (Fluke 8846A). Calculated volumes[5] of liquids were injected into the chamber using a microliter pipette. Sensitivity (S), was calculated using Eq. (1), where R_a and R_g correspond to samples' resistance in air and in presence of target gas, respectively:[8]

$$S = \frac{R_a - R_g}{R_g} \times 100. \qquad (1)$$

Figure 1 shows the TEM images of the ZnO samples prepared using two lasers ("ns" and "ms" stand for nanosecond and millisecond pulses). The samples are seen to exhibit two contrasting morphologies, nanospheres and
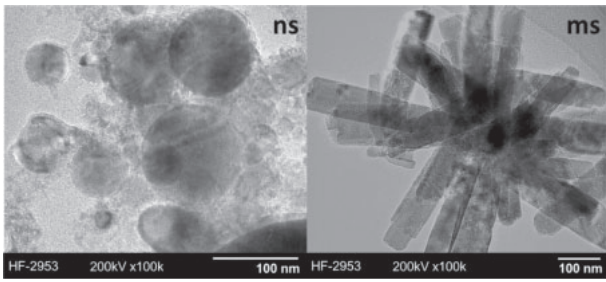
Fig. 1. TEM images of ZnO nanospheres and nanorods prepared using ns and ms pulsed lasers.

nanorods, respectively. The average size of the former NPs is ~30–50 nm, while the latter are <300 nm in length. Longer pulses (ms-laser) are known to increase the temperature of liquid medium.[9–11,14] This was confirmed by the present study, as the nanospheres and nanorods in Fig. 1 were prepared in water at 25 and 65 °C, respectively. In accordance with the previous reports, because the initially formed ZnO NPs could then agglomerate and re-crystallize in the surrounding medium, the increased medium temperature during preparation led to nanorod formation when ms pulsed laser was used.[10,12] This explains why the ZnO NPs generated by ns-laser remained spherical [Fig. 1(a)], while their counterparts in Fig. 1(b) crystallized as ZnO nanorods.

Figure 2 shows the XRD patterns of both ZnO samples prepared using two different lasers. The diffraction peaks observed at 31.7, 34.3, and 36.1° correspond to the (100), (002), and (101) planes, respectively, thus revealing formation of hexagonal wurtzite crystal structures, in good agreement with standard pattern (JCPDS 36-1451). The peak intensities observed in Fig. 2 imply that the crystallinity of the nanospheres is higher than that of the nanorods.[24] The intensity ratio ($I_{(002)}/I_{(101)}$) of standard ZnO pattern is known to be 0.44.[25,26] At the same time, the patterns in Fig. 2 show such values as 0.49 and 0.79, the latter value revealing that the ZnO nanorods are preferably c-axis oriented.
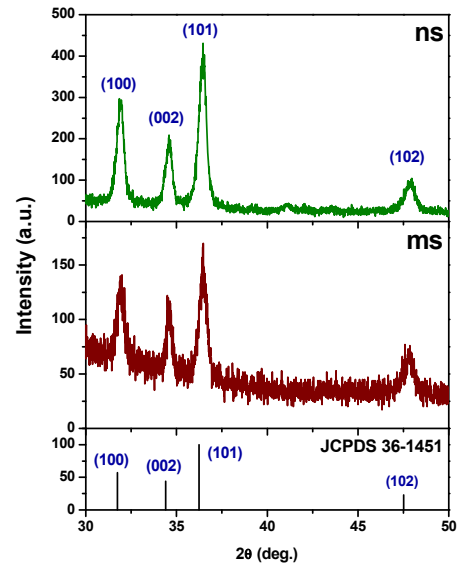
Fig. 2. (Color online) XRD patterns of ZnO samples prepared using ns and ms pulsed lasers.

Figure 3(a) shows the response of ZnO nanospheres and nanorods towards 250 ppm of ethanol, ammonia and acetone at room temperature (20 °C). It is well seen that the ZnO nanospheres exhibited both a high response and selectivity towards ethanol. This might be due to the combination of their higher crystallinity, NP size and densely packed morphology with high surface area formed on electrode.[8,25,26] Figure 3(b) shows a dynamic-response curve of ZnO nanospheres towards different ethanol concentrations. It is clearly seen that the material can detect ethanol in the range 50–250 ppm with sensitivity values between ~7 and 19. The linear increase in the response implies the availability of active surface sites for the adsorption of ethanol molecules.[17] Smaller ethanol concentrations (1, 10, and 25 ppm) were also tested, resulting in noisy response. It is known that the ethanol dissociation energy, operation temperature and
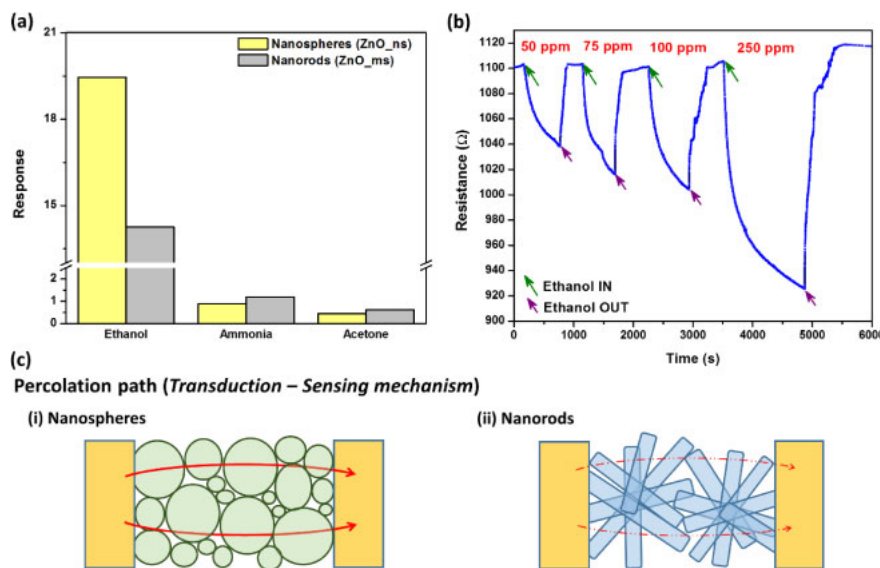
Fig. 3. (Color online) (a) Sensing response of ZnO nanospheres and nanorods towards 250 ppm of ethanol, ammonia, and acetone, as measured at room temperature. (b) Dynamic-response curve of ZnO nanospheres towards different concentrations of ethanol. (c) Percolation path threshold in the two gas sensors based on ZnO nanospheres and nanorods.

Table I.   Sensing performance of LAL-prepared nanomaterials.

Sample	Target gas	Concentration (ppm)	Operating temperature (°C)	Sensitivity	Source
ZnO nanospheres	Ethanol	250	20	19	This work
ZnO nanorods	Ethanol	250	20	14	
WO$_3$ nanoflakes	Ethanol	600	250	11	Ref. 15
		600	150	7	
ZnS hollow NPs	Ethanol	10	200	1.5[a]	Ref. 9
	Acetone	10	200	1.15[a]	

a) Sensitivity $= R_a/R_g$.

sensing material (its surface defects, morphology and chemistry) define the detection limit of ethanol,[6] which is why it can be expected that further optimisation of the sensor based on LAL-generated ZnO can lead to lower detection limits.

Oxygen adsorption from the atmosphere is known to result in trapping of conduction electrons on the surface and formation of a depletion layer.[5,7,25,27] This hinders the flow of electrons across junctions in the nanomaterial (sensor), leading to an increase in resistance of the sensing element (baseline resistance). When reducing gas molecules (e.g., ethanol) interact with such chemisorbed oxygen, the latter oxygen gets reduced [Eqs. (2) and (3)], which leads to a decrease in surface resistance.

$$O_{2(atmosphere)} + e_{(ZnO\ surface)}^{-} \rightarrow O_{2(ZnO)}^{-} \qquad (2)$$

$$C_2H_5OH + 3O_{2(adsorbed)}^{-} \rightarrow 2CO_2\uparrow + 3H_2O\uparrow + 3e^-\downarrow \quad (3)$$

The sorption process depends heavily on the surface properties, such as defect density and nature, surface morphology, etc. Both ZnO morphologies studied in this work showed selective response towards ethanol [Fig. 3(a)], with that of the nanospheres being higher. Although there may be many other parameters contributing to the higher sensitivity, it is believed that the percolation path (i.e., path of electrons across junctions) is more favorable in the case of nanosphere-based sample due to network of intergranular contacts.[27] Figure 3(c) shows schematically how electrons travel between electrodes across the two sensing devices prepared in this study (so-called "percolation threshold"[27]). Another important parameter might be the better crystallinity detected in the nanospheres by XRD.

Table I compares the results obtained in this study with those reported by others for gas sensing performance of LAL-prepared nanomaterials.[9,15] The nanostructures reported in this study are seen to compare well with other devices that use LAL-generated nanomaterials. Importantly, they operate at room temperature, and ethanol concentration of 50 ppm could be easily detected. Overall, LAL-prepared nanomaterials are seen as promising materials for gas sensing, and their further optimization, through better understanding of morphology effect, in-situ doping and tuning product properties via laser and medium parameters, is expected to result in development of new efficient sensors for different volatile organic compounds.

In conclusion, nanomaterials of ZnO with two different morphologies, nanospheres and nanorods, were prepared by ablating Zn plates in water with nanosecond- and millisecond-pulsed lasers, respectively. For the first time, chemiresistive sensing devices prepared using the two nanomaterials were tested with ammonia, ethanol and acetone,

exhibiting selective response towards ethanol at room temperature. The combinational effect of dissociation energy of ethanol, higher crystallinity of particles and efficient percolation paths is believed to be responsible for the enhanced sensing response of the ZnO nanospheres at room temperature. It is thus proved that laser-generated nanomaterials can be promising for developing gas sensing elements capable of detecting at room temperature.

1) I. D. Kim, A. Rothschild, and H. L. Tuller, Acta Mater. **61**, 974 (2013).
2) Y. Q. Zhang, Z. Li, T. Ling, S. A. Kulinich, and X. W. Du, J. Mater. Chem. A **4**, 8700 (2016).
3) N. Barsan, D. Koziej, and U. Weimar, Sens. Actuators B **121**, 18 (2007).
4) N. Yamazoe and K. Shimanoe, J. Sens. **2009**, 875704 (2009).
5) P. Shankar and J. B. B. Rayappan, ACS Appl. Mater. Interfaces **8**, 24924 (2016).
6) N. Bârsan, Sens. Actuators B **17**, 241 (1994).
7) X.-H. Liu, P.-F. Yin, S. A. Kulinich, Y.-Z. Zhou, J. Mao, T. Ling, and X.-W. Du, ACS Appl. Mater. Interfaces **9**, 602 (2017).
8) P. Shankar and J. B. B. Rayappan, RSC Adv. **5**, 85363 (2015).
9) K. Y. Niu, J. Yang, S. A. Kulinich, J. Sun, and X. W. Du, Langmuir **26**, 16652 (2010).
10) M. Honda, T. Goto, T. Owashi, A. G. Rozhin, S. Yamaguchi, T. Ito, and S. A. Kulinich, Phys. Chem. Chem. Phys. **18**, 23628 (2016).
11) K. Y. Niu, J. Yang, S. A. Kulinich, J. Sun, H. Li, and X. W. Du, J. Am. Chem. Soc. **132**, 9814 (2010).
12) Y. Ishikawa, Y. Shimizu, T. Sasaki, and N. Koshizaki, J. Colloid Interface Sci. **300**, 612 (2006).
13) Z. Yan and D. B. Chrisey, J. Photochem. Photobiol. C **13**, 204 (2012).
14) H. B. Zeng, X. W. Du, S. C. Singh, S. A. Kulinich, S. K. Yang, J. P. He, and W. P. Cai, Adv. Funct. Mater. **22**, 1333 (2012).
15) J. Xiao, P. Liu, Y. Liang, H. B. Li, and G. W. Yang, Nanoscale **4**, 7078 (2012).
16) S. A. Kulinich, T. Kondo, Y. Shimizu, and T. Ito, J. Appl. Phys. **113**, 033509 (2013).
17) T. Goto, Y. Shimizu, H. Yasuda, and T. Ito, Appl. Phys. Lett. **109**, 023104 (2016).
18) X. Zhou, Q. Xue, H. Chen, and C. Liu, Physica E **42**, 2021 (2010).
19) X. Zhou, Q. Xue, M. Ma, and J. Li, Thin Solid Films **519**, 6151 (2011).
20) H. J. Pandya, S. Chandra, and A. L. Vyas, Sens. Actuators B **161**, 923 (2012).
21) P. Shankar and J. B. B. Rayappan, Sens. Lett. **11**, 1956 (2013).
22) I. Muniyandi, G. K. Mani, P. Shankar, and J. B. B. Rayappan, Ceram. Int. **40**, 7993 (2014).
23) A. J. Kulandaisamy, C. Karthek, P. Shankar, G. K. Mani, and J. B. B. Rayappan, Ceram. Int. **42**, 1408 (2016).
24) A. Goux, T. Pauporte, J. Chivot, and D. Lincot, Electrochim. Acta **50**, 2239 (2005).
25) G. K. Mani and J. B. B. Rayappan, Sens. Actuators B **223**, 343 (2016).
26) K. Sivalingam, P. Shankar, G. K. Mani, and J. B. B. Rayappan, Mater. Lett. **134**, 47 (2014).
27) M. Ulrich, A. Bunde, and C.-D. Kohl, Appl. Phys. Lett. **85**, 242 (2004).